Improving geometric quality of laser machined parts using high-precision motion system dynamic performance analysis

Bordatchev, Evgueni V.; Nikumb, Suwas

Publisher's version / Version de l'éditeur:

Proceedings WMC'2001, 2001

IMPROVING GEOMETRIC QUALITY OF LASER MICROMACHINED PARTS USING HIGH-PRECISION MOTION SYSTEM DYNAMIC PERFORMANCE ANALYSIS

Evgueni V. Bordatchev* and Suwas K. Nikumb

Integrated Manufacturing Technologies Institute, National Research Council of Canada
800 Collip Circle, London, Ontario, Canada N6G 4X8

ABSTRACT

Dynamic performance of the motion system is a key element for achieving the highest accuracy and precision of parts from a particular laser micromachining system. This paper describes an analysis of the dynamic performance of a high-precision motion system and its relevance to the improvement in geometric quality of the machined parts. The dynamic and statistical parameters of motion are utilized to evaluate the dynamic performance of the entire motion system. Also, experimental results applied to high-precision laser micromachining allow significant improvements in the precision and quality of the machined parts. An example of a micromachined line pattern on a flexible circuit board is presented. Better geometric quality in machined parts with increased precision in the track width, from +/- 2.20 μm up to +/- 0.75 μm, was obtained. The results highlight sources of improvement in the part geometric quality and the laser micromachining process.

INTRODUCTION

The laser micromachining system is a complex electro-optical-mechanical system [1-3], consisting of the laser/optics and the workpiece motion system as subsystems. The motion system is an important part of a laser micromachining system, where precise movement of the workpiece plays an important role in the final dimensions of the machined part. The ideal laser machining system must provide an adequate conformance of the laser beam focal spot on the workpiece surface in accordance with the predetermined tool path. However, laser-machining experiments [1-6] indicate that the geometric qualities of the machined workpiece are not only defined by the predetermined tool path and process parameters, but also are influenced by the dynamic processes that occur during machining. These dynamic processes are (a) travel motions of a workpiece, (b) space-time fluctuations in the laser beam parameters, and (c) laser-material interactions. Among these processes the non-uniformity of motion is a major factor in the formation of final geometric quality of laser-machined parts. A combination of kinematic (e.g., geometrical errors) and dynamic (e.g., frictional process) disturbances produces uneven travel motions and affects the synchronization with the individual laser beam pulses. Modern laser micromachining is based on CNC technology, where recent activities in improving the geometric quality of the machined parts are targeted on better positional accuracy of the motion system and reducing tracking error [7]. These activities are based on modifications of control systems and do not involve the consideration of how dynamic individuality of specific motion system affects final geometric quality of machined parts.

This paper describes a method to improve geometric quality of laser micromachined parts by selecting an appropriate combination of motion (travel speed) and laser parameters (focal spot diameter, frequency of laser pulses). Particularly, the dynamic performance of the entire high-precision motion system is analyzed on the basis of the non-uniformity in motion translation within the travel envelope. The dynamic and statistical parameters and characteristics of a specific motion are explored to evaluate the dynamic performance as the "dynamic imprint" of the motion system. Application of the results of analysis to a high-precision laser micro-machining system provided significant improvement in the precision and quality of the machined parts. An example of a micro-machined line pattern on a flexible circuit board is presented. A better geometric quality was obtained within the tolerance of the track width from +/- 2.20 μm to +/- 0.75 μm. These results indicate the applicability of this concept for a wide range of industrial applications such as certification, diagnostics, and tool path optimization.

CONCEPT of LASER MICROMACHINING

The laser micromachining is a process where a laser beam acts as a tool and removes material from a workpiece in accordance with a specified tool path [1-3]. The laser micromachining system is a complex electro-optical-mechanical system consisting of:

- the laser/optics as a subsystem, which delivers the laser beam into the processing zone
- the workpiece motion subsystem, which includes a base, electro-drives, and translation stages to provide the travel motions accordingly to the CNC tool path.

During the machining process, multiple pulses are applied to the same location for material removal applications. Controlled depth or blind pocket micromachining utilizes control of the pulse duration and the energy per pulse to instantaneously vaporize a known quantity of the material

* Corresponding author. Tel.: 1-519-430-7107; fax: 1-519-430-7064; e-mail: evgueni.bordatchev@nrc.ca

from the workpiece surface. Controlling the number of layers machined controls the machined depth. Figure 1 shows the schematics of the laser micromachining path.

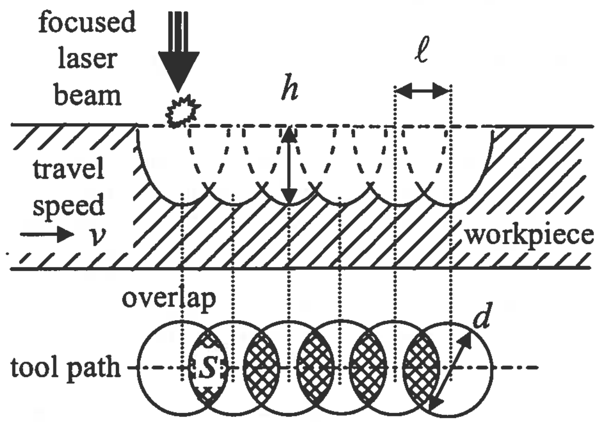

Fig. 1. Schematics of the laser micromachining path.

A set of laser machining parameters can be defined to help clarify the method used in this work: E - the pulse energy (J); f_{ls} - the frequency of laser pulses (Hz); d - the focal spot diameter (mm), assuming that the focal spot is circular for TEM00 mode; and v - the travel speed (mm/s). Each laser pulse vaporizes a certain amount of material and creates a dent into the workpiece material. The dent profile is approximated by a cylindrical paraboloid with a height h (machined depth for one path), diameter d, and volume $V = \pi d^2 h/2$. A combination of these dents along the tool path defines the geometry of the machined part. The ideal part geometry can be achieved when the process parameters (E, f_{ls}, d, v) are constant and correspond to constant one-dimensional overlap S (%) between two consecutive pulses. The spot overlap is calculated by

$$S = 100\% \times (d - \ell)/d = (1 - \ell/d) \times 100\%, \qquad (1)$$

where ℓ is the distance between two consecutive dents/pulses and $\ell = v/f_{ls}$ (mm).

It is clear from expression (1) that spot overlap depends upon the selection of frequency of laser pulses (f_{ls}) and travel speed (v) for a given focal spot diameter (d), which directly relates to the pulse energy (E). Any variation within each parameter will change the spot overlap (S) and volume of material removed (V) and concomitantly the geometric quality of the machined part. The laser is a fairly stable dynamic system and the variation of the pulse energy lies within +/- 5%. Therefore our investigations are mainly focused on non-uniformity within the travel speed.

EXPERIMENTAL SETUP AND METHOD

Figure 2 shows the experimental setup used for the measurements. A multi-axis positioning system was used for the signal measurements and data collection. The worktable consists of a granite base fitted with precision translation stages (with air bearings) for X and Y movements. The linear motors LM210-16.80-3-AC (Trilogy Systems Corp.) provide the feed motion, and the corresponding LS403 linear encoders (HEIDENHAIN Corp., resolution 0.5 μm) furnish the positional feedback for the control system. The data related to linear motion was acquired using a PCI-MIO-16XE-10 (National Instruments™) I/O card. All measurements were carried out for 50 *mm* feed movement in X and Y directions for a wide range of travel speeds from 2.54 *mm/s* – 50.8 *mm/s* in acceleration phase and in steady-state phase. The design peculiarity of this motion system is that the Y-axis stage is located on the top of X-axis stage.

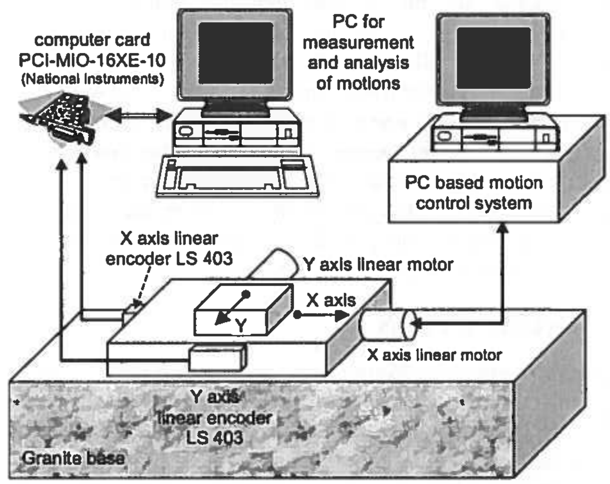

Fig. 2. Schematic diagram of the experimental setup.

The travel speed is measured by using a time-based measurement technique, which consists of measuring each time period T_i (s) of the impulse sequence from the position encoder, where i is the number of impulses produced by the position encoder. Therefore the travel distance x (mm) corresponds to $i = 1:k$ steps, with a length of encoder resolution λ which in our case is 0.5 μm. It is important to note that time-based measurement of the period $T(x)$ does not limit the obtainment of values for the travel distance $x(t)$ and speed $v(t)$ as functions of time.

The time-based measurement technique provides original information about the travel motion, regarding the measured impulse period $\hat{T}(1:k)$, where k is the number of measured impulses. Each value of $\hat{T}_i$ is represented by the number of pulses with frequency f_{hf} and period

$T_{hf} = 1/f_{hf}$ which occur during the actual period T_i, $i = 1:k$. Based on the original information $\hat{T}(1:k)$ the following processes can be computed precisely:

a) "periods with respect to position" process $T(x)$, which represents the actual interval value for the specified position and can be calculated based on $\hat{T}(1:k)$ and T_{hf} as

$$T(x) = \hat{T}(1:k) \times T_{hf}, \quad x = (1:k) \times \lambda \qquad (2)$$

b) "travel speed with respect to position" process $v(x)$, which represents the actual travel speed for the specified position and can be calculated based on $T(x)$ and λ as

$$v(x) = \lambda / T(x), \quad x = (1:k) \times \lambda \qquad (3)$$

c) "travel speed with respect to time" process $v(t)$, which represents the time behavior of the travel speed and can be calculated based on $v(x)$ and $T(x)$ as

$$v(t) = v(x), \quad t_i = \sum_{j=1}^{i} T_j, \quad i = 1:k \qquad (4)$$

Note that $v(t)$ and $v(x)$ processes have equal amplitudes. The difference between $v(t)$ and $v(x)$ is that $v(t)$ represents the behavior of travel speed in the time domain and $v(x)$ in the space domain. These two processes clearly represent two different domains of the original motion; however, for the determination of process behavior, the statistical analysis can be applied only to "travel speed with respect to position" process $v(x)$, which has an even scale in space because of constant interval λ.

d) "position with respect to time" process $x(t)$ represents the time behavior of motion and can be obtained from $T(x)$ as

$$x_i = i \times \lambda, \quad t_i = \sum_{j=1}^{i} T_j, \quad i = 1:k \qquad (5)$$

The information obtained from the above analysis opens up a wide range of engineering applications for diagnostics, control, optimization and prediction of the dynamic performance of the motion system. It is also important to note that the information about the dynamic performance of the motion system and sources of disturbances can be obtained using the comparison between the time and space processes. For example, the dynamic and kinematic disturbances can be separated modifying the motion system dynamics, since the spatial locations of the kinematic disturbances remain unchanged.

Analysis of the motion system dynamic performance includes the following steps and operations:

a) Set up parameters: distance of motion, L (*mm*); predetermined travel speed, v_0 (*mm/s*); encoder resolution, λ

b) Calculate $k = L/\lambda$, which is the number of pulses produced by the position encoder for motion distance of L

c) Run motion system and measure "period with respect to position" process $\hat{T}(1:k)$

d) Calculate and represent graphically:
   - original (measured) data $\hat{T}(1:k)$
   - "period with respect to position" process $T(x)$ based on expression (2)
   - "travel speed with respect to position" process $v(x)$ based on expression (3)
   - "travel speed with respect to time" process $v(t)$ based on expression (4)
   - "position with respect to time" process $x(t)$ based on expression (5)

e) calculate statistical parameters, which characterize the actual technical state and dynamic quality:
   - highest, v_{max}, and lowest, v_{min}, values of $v(x)$
   - amplitude of travel speed fluctuations, $A_v = v_{max} - v_{min}$ (*mm/s*)
   - mean value of travel speed μ_v (*mm/s*)
   - coefficient of non-uniformity, K_v, which shows relative amplitude of fluctuations, as

$$K_v = (v_{max} - v_{min}) / \mu_v \times 100\% \qquad (6)$$

   - variance of travel speed, σ_v^2 ($(mm/s)^2$), which estimates fluctuations in general
   - and difference $\mu_v - v_0$, which estimates level of technical perfection.

Of course, the list of suggested statistical parameters can be extended further for evaluating probability distribution function, standard deviation, autospectral density function, autocorrelation function and so on; however, the usefulness of these characteristics will depend on the specific engineering application.

RESULTS AND DISCUSSION

Analysis of accelerated motions

Significant loss of accuracy and quality occurs in laser micromachining at the start- and end-point of the tool path, which corresponds to acceleration and deceleration of the stages. This is because there is no synchronization between the motion and laser pulses. Figure 3 shows accelerated motion at the start point, where the depth (21 *μm*) of the start-point is three times more than the depth achieved during the steady-state motion (7 *μm*). Accelerated motion takes place during the acceleration phase when travel speed changes to reach a value predetermined by the NC program; for example, when the motion system begins to move from an initial point.

According to the control theory [8], the acceleration phase is called "step response" and is one of the most important system characteristics representing the dynamic quality of the motion system.

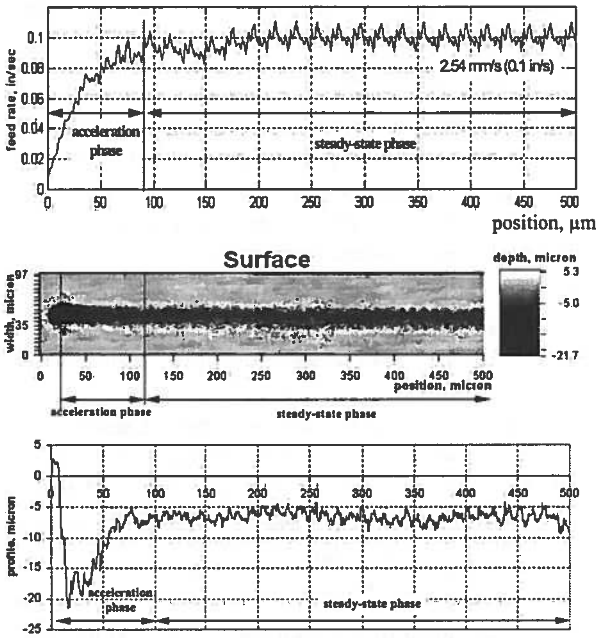

Fig. 3. Accelerated motion and corresponded surface profile at the start point.

Figure 4 illustrates the observed accelerated motion for different travel speeds ranging from 2.54 *mm/s* to 12.7 *mm/s* for X and Y axes. Analysis of the accelerated motion plays a significant role for the tuning of the control system. Both figures illustrate the evolution of the acceleration phase and its behavior. The curve of the acceleration phase changes with an increase in the travel speed value. For example, the all curves for X-axis have overshoot and oscillations around the steady-stage travel speed. Otherwise, the curves for Y-axis have an exponential growth character without any overshoot or oscillations. This difference will cause different tracking and positioning errors in engineering applications. It is also clear that the motion system has a different dynamic performance for various travel speeds.

In addition, the length of the acceleration phase increases with an increase in the travel speed. This performance is certainly not a surprise from the control theory point of view, but is very important for the prediction of the geometric quality of the laser-machined parts. The length of the acceleration phase determines the distance where very poor geometric quality is expected. Therefore for practical applications and experiments the laser could be switched-on after the acceleration phase. Table 1 shows the length of acceleration phases for different travel speeds and motion directions, where the data was extracted from Fig. 4 based on criteria of the automatic control theory [8]. It is also necessary to note that for the same travel speeds the length of the acceleration phase is different for different axes, e.g., for travel speed 12.7 *mm/s* the length is 0.53 *mm* for X axis and 1.03 *mm* for Y axis.

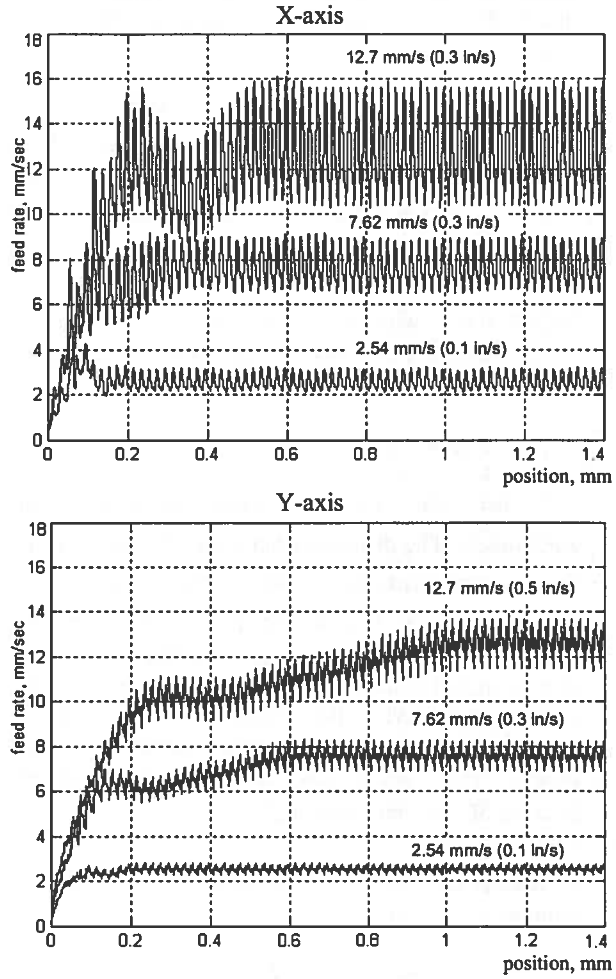

Fig. 4. Accelerated motions.

Table 1. Lengths of acceleration phase (*mm*) for different travel speeds and directions of motion

	Travel speed, *mm/s*		
	2.54	7.62	12.7
X axis	0.19	0.32	0.53
Y axis	0.22	0.61	1.03

Because the control systems for both axes are identical, there are two possible explanations:

- By design, the Y stage is located on the top of the X stage, which provides different dynamics for each stage.
- The tuning parameters of the motion controllers are different.

These facts should be taken into account to understand

and predict the dynamic performance and corresponding geometric quality during laser micromachining.

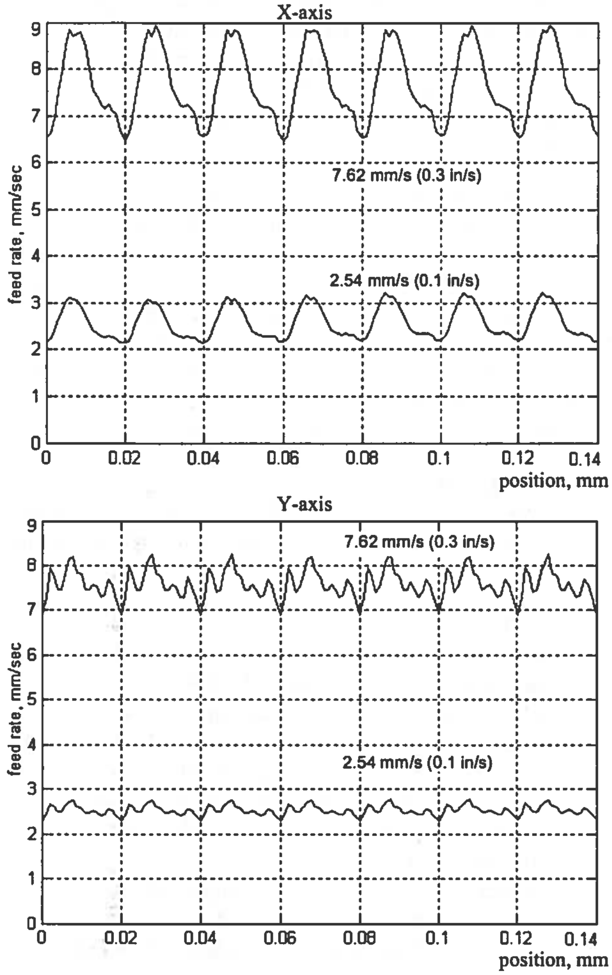

Fig. 5. Steady-state motions.

Analysis of steady-state motions

After the acceleration phase, the motion reaches a steady-state condition, where the control system provides a minimum deviation of travel speed around the predetermined tool path value, which also corresponds to the synchronized mode of laser micromachining. In this phase, the control system reacts mainly to external and internal disturbances, which resist the motion. Figure 5 illustrates the observed steady-state motions for different travel speeds - 2.54 *mm/s* and 7.62 *mm/s* for X and Y axis. Analysis of the steady-state motion signatures is also important because the behavior of motion clearly represents the ability of a control system to respond to and compensate for dynamic and kinematic disturbances. It is well known that the frequency range of the actual disturbances is wider than that of the control system. Therefore, control algorithms cannot effectively compensate for these high-frequency disturbances. Figure 5 clearly illustrates this issue where variations of the travel speed with a period of 20 μm and less do exist. These variations were expected because it is known [9, 10] that actual travel motions for any real mechanical system have uneven and non-uniform character due to external and internal kinematic and dynamic disturbances, (e.g. geometric and kinematic errors, assembly errors, friction forces, process forces, *etc*), which cause resistance to motion. Therefore, analysis of the steady-state motion is effective for identification of sources and further compensation of disturbances.

Obtaining the motion parameters, which estimate the non-uniformity, is a significant part of the analysis of the motion system's dynamic performance. Therefore the values of feed motion parameters such as highest v_{max} and lowest v_{min} values, mean value μ_v, coefficient of non-uniformity K_v, variance σ_v^2, and difference $\mu_v - v_0$ are calculated for travel speeds from 2.54 *mm/s* to 12.7 *mm/s*. The results of the calculations are presented in Tables 2 and 3 for X- and Y-axis respectively. Detailed analysis of these results shows that the motion system under consideration has different technical perfection and dynamic performance for X- and Y-axis. The following factors support these conclusions:

- The Y axis motions achieve predetermined travel speed; where as the X motions did not. This means that the Y motion subsystem has better technical perfection than the X motion subsystem. The difference $\mu_v - v_0$ is the parameter that estimates the technical perfection.
- The amplitude of the travel speed fluctuations, A_v, linearly increases with a corresponding increase in the predetermined travel speed, resulting in a decrease in the overall system performance. The amplitude A_v for X motion is also bigger than for Y motion within the equal predetermined travel speed. This indicates that the dynamic performance of the Y motion subsystem is better than that of the X motion subsystem.
- For both axes, the variance σ_v^2 increases exponentially as the travel speed increases. The variance σ_v^2 for X motion is bigger than for Y motion within the equal predetermined travel speed. This also indicates that the dynamic performance of the Y motion subsystem is better than that of the X motion subsystem.
- The amplitude A_v and variance σ_v^2 are the parameters that estimate the dynamic performance of the motion system. These parameters complement each other, and only a compromise between them provides optimal motions, correspondingly achieving highest accuracy for the particular motion system.

- Coefficient of non-uniformity K_v remains relatively constant for all travel speeds and both axes, and it cannot reasonably characterize the system performance for different travel speeds.

In addition, Figure 5 shows that although changing travel speeds means changing the dynamics of the motion system, the signature of individual motion does not change. Fluctuations have repetitive shapes and constant periods of 20 μm; the amplitude of motion fluctuations increases correspondingly with the increase in travel speed, resulting in a decrease in the overall system performance. These motion signatures, which are not related to the system dynamics, clearly indicate the presence of kinematic disturbances within the motion system.

The analysis described above was applied to a high-precision laser micromachining system in our laboratory. The system consists of an electro-optically Q-switched, diode pumped, solid-state laser (model HPO-1000, Continuum Inc.) with an appropriate beam delivery system and a CNC-based, high-precision, three-axis positioning system. Using such a system a micro-line pattern was machined on a standard flexible circuit board. The conductor width, as well as the spacing between two conductors, was chosen to be 20 μm. The length of the pattern lines was 20 *mm*. Figure 6 illustrates the conductor lines machined along Y and X directions respectively. It is clear that the lines machined along the X-axis are much wavier at the edges than those machined along the Y-axis. An optical microscope "Olympus" (model PMG 3) was utilized to measure the width deviation of the machined lines. It was observed that the Y-lines have a width of 20.0 +/- 0.75 μm, and the lines machined along the X-axis have a width of 20.0 +/- 2.20 μm, indicating an increase in the precision of machined lines by a factor of three, e.g. in the track width from +/- 2.20 μm up to +/- 0.75 μm. The results show that the relationship between the direction of motion and the use of the above analysis of non-uniformity allows the selection of a more appropriate tool path direction and workpiece orientation to provide better part quality.

SUMMARY AND CONCLUSIONS

In order to improve the geometric quality of laser machined parts the dynamic performance of the high-precision motion system has been analyzed. The results of the analysis allowed a factor of three increase in precision in the production of a micro-line pattern on standard flexible-circuit board, e.g. increased precision in the track width from +/- 2.20 μm up to +/- 0.75 μm. The statistical parameters of motion, such as difference between process mean value and predetermined travel speed, coefficient of non-uniformity, and variance, to characterize the actual technical state, the dynamic quality, and the level of technical perfection of the motion system, have been evaluated. The time-based technique was applied to measure the motion as a space-time random process. It consists of the measurement of the time duration of periods produced from the positional encoder. Motions with different travel speeds were investigated in order to compare the dynamic performance.

Dynamic performance is a key element to achieve high accuracy and precision from a particular motion system. The statistical parameters and characteristics of motion are most appropriate indicators of the dynamic performance and represent a "dynamic imprint" of the motion system. Experimental results show that the analysis of the high-precision motion system's dynamic performance highlights sources of improvement in part geometric quality from the laser micromachining process.

ACKNOWLEDGMENT
The authors greatly appreciate the support of Mr. Hugo Reshef and Mr. Craig Dinkel for their assistance in conducting the experiments.

REFERENCES

1 W.M. Steen, Laser Material Processing, 2nd edition, Springer-Verlag, New York, NY (1998).
2 G. Chryssolouris, Laser Machining: Theory and Practice, Springer-Verlag, New York, NY (1991).
3 E.V. Bordatchev and S.K. Nikumb, "Laser material-removal process as a subject of automatic control," Proc. of the ASPE 14th Annual Meeting, Monterey, California, USA, (1999) 236-239.
4 J.J. Chang, B.E. Warner, E.P. Dragon, M.W. Martinez, "Precision micromachining with pulsed green lasers," J. of Laser Applications, 10, 6 (1998) 285-291.
5 S.K. Nikumb and M.U. Islam, "High-precision machining of materials for manufacturing applications using diode pumped solid state lasers," High-Power Lasers in Manufacturing, Proceedings of the SPIE, Vol. 3888 (2000) 188-197.
6 F. Dausinger, "Drilling of high quality micro holes," Proceedings of the Laser Materials Conference ICALEO-2000, LIA Vol. 89 (2000) 1-10.
7 K. Srinivasan and T.C. Tsao, Machine tool feed drives and their control - A survey of the state of the art. J of Manuf Sc and Eng, 119, 1997, pp. 743-748.
8 B. C. Kuo, Automatic control systems. 6th ed., Prentice Hall, 1991.
9 H.Z. Bin, K. Yamazaki, M.F. DeVries, A stochastic approach to the measurement and analysis of leadscrew drive kinematic errors. J of Eng for Ind, 106, 1984, pp. 339-344.
10 S.R. Postlethwaite, D.G. Ford, D. Morton, Dynamic calibration of CNC machine tools. Int J Mach Tools Manuf, 37(3), 1997, pp. 287-294.

Table 2. Steady-stage motion parameters for different travel speeds (X axis)

v_0, *mm/s*	v_{max}, *mm/s*	v_{min}, *mm/s*	A_v, *mm/s*	μ_v, *mm/s*	$\mu_v - v_0$, *mm/s*	K_v, %	σ_v^2, $(\mu m/s)^2$
2.54	3.33	2.11	1.22	2.59	0.05	47.10	0.28656
7.62	9.17	6.25	2.92	7.70	0.08	37.92	1.41588
12.70	16.13	10.31	5.82	12.90	0.20	45.12	6.92094

Table 3. Steady-stage motion parameters for different travel speeds (Y axis)

v_0, *mm/s*	v_{max}, *mm/s*	v_{min}, *mm/s*	A_v, *mm/s*	μ_v, *mm/s*	K_v, %	σ_v^2, $(\mu m/s)^2$
2.54	2.90	2.18	0.72	2.54	28.35	0.03806
7.62	8.48	6.53	1.95	7.62	25.59	0.26902
12.70	14.10	11.23	2.87	12.70	22.60	0.75285

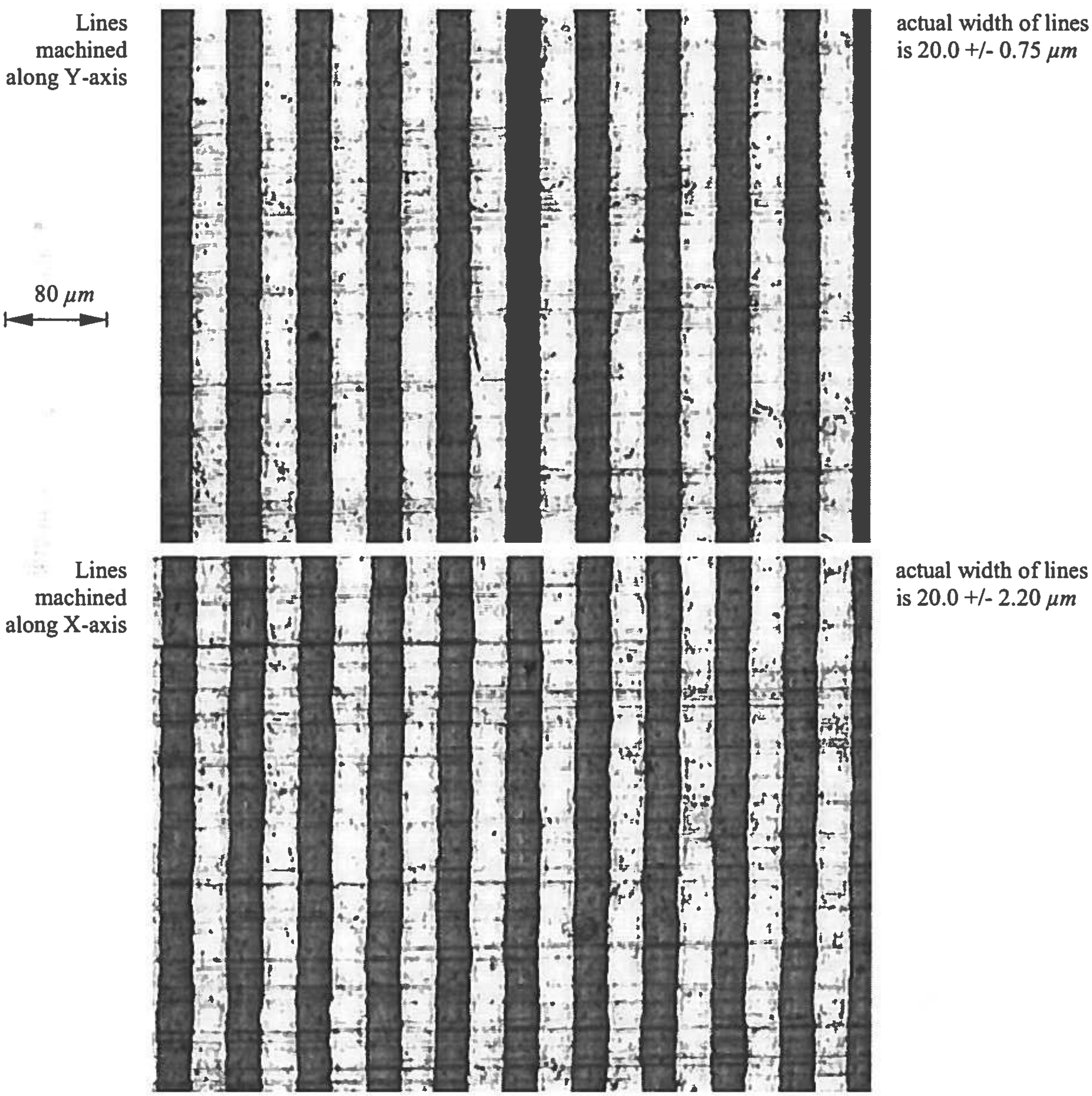

Fig. 6. Machined copper lines with a desired width of 20.0 μm.